

NONLINEAR SCALE-LOCAL DEFORMATIONS OF VORTEX RINGS IN SMOOTH EULER FLOWS

TSUYOSHI YONEDA

ABSTRACT. We consider the incompressible three-dimensional Euler equations in a setting where a vortex ring undergoes radially expanding Lagrangian transport. To clarify the fundamental mechanisms responsible for nonlinear scale-local deformations of the vortex structure, we develop a geometric Lagrangian framework that avoids singular integral representations of the pressure and leads to the derivation of a novel wave equation governing the axis of swirling particles. Within this framework, we identify purely nonlinear mechanisms responsible for the emergence of scale-local deformations of the vortex structure, with the aid of a machine-learning-based analysis.

1. INTRODUCTION

One of the most important features of Navier–Stokes turbulence is that it is not random but is instead organized around vortex-stretching dynamics. More precisely, recent direct numerical simulations of Navier–Stokes turbulence at sufficiently high Reynolds numbers [2, 3, 11, 12] have reported the existence of a hierarchical structure of vortex-stretching motions. In particular, Goto–Saito–Kawahara [3] clearly observed that turbulence at sufficiently high Reynolds numbers in a periodic cube exhibits a self-similar hierarchy of antiparallel vortex-tube pairs, which is sustained by the generation of smaller-scale vortices through stretching within larger-scale strain fields. This observation was further investigated by Y–Goto–Tsuruhashi [15] and Tsuruhashi–Goto–Oka–Y [14] (see also [5, 6, 7] for related mathematical results). Following this line of research, attention naturally turns to the scale-local deformations of vortical structures, which play a central role in the energy cascade.

A natural setting in which such scale-local deformation mechanisms can be examined in a controlled manner is provided by the collision of vortex rings. Many studies have investigated vortex-ring collisions (see [10] and references therein), and the main findings can be summarized as follows. When two vortex rings of equal strength and opposite circulation collide head-on, a strong strain field is generated. It is well known that the dominant instability mechanism depends on the Reynolds number. At low Reynolds numbers, long-wavelength Crow-type instabilities prevail, leading to relatively mild deformations. In contrast, at high Reynolds numbers, short-wavelength perturbations at the scale of the vortex core radius become dominant, and the dynamics are governed by the elliptical instability. However, the elliptical instability is derived from a linear stability analysis and does not, by itself, provide a rigorous description of the nonlinear evolution.

Date: February 5, 2026.

2010 Mathematics Subject Classification. Primary 35Q31; Secondary 76B47; Tertiary 76B55.

Key words and phrases. Euler equations, Frenet–Serret formulas, Optuna.

With this perspective in mind, in this paper, we develop a geometric Lagrangian framework for the three-dimensional incompressible Euler equations that avoids singular integral representations of the pressure. Within this framework, we rigorously derive a novel wave equation governing the evolution of the axis of swirling particles, and we further employ a machine-learning-based analysis to identify purely nonlinear mechanisms responsible for the emergence of scale-local deformations of the vortex structure.

2. DERIVATION OF A NOVEL WAVE EQUATION

Let Φ denote the Lagrangian flow map associated with the incompressible Euler equations, written in Lagrangian form (omitting the explicit volume-preserving constraint) as follows:

$$(1) \quad (\partial_t^2 \Phi(t, \cdot)) \circ \Phi^{-1}(t, x) = -\nabla p(t, x), \quad t > 0, \quad x \in \mathbb{R}^3.$$

Let $\ell = \bigcup_s \ell(s) \subset \mathbb{R}^3$ be a smooth curve representing the vortex axis. We now describe the time evolution of swirling particles around ℓ . Let z denote the arc-length parameter along the transported curve $\bigcup_t \Phi(t, \ell(s))$. More precisely, we define a reparametrization $t = t(z)$ (implicitly depending on s) by

$$(2) \quad \partial_z t = v(t)^{-1} \quad v(t) := |\partial_t \Phi(t, \ell(s))|,$$

so that

$$|\partial_z \Phi(t(z), \ell(s))| = 1.$$

Note that this implies $\partial_z = v(t)^{-1} \partial_t$. Using the transported curve $\bigcup_t \Phi(t, \ell(s))$, we introduce a Lagrangian moving frame. First, we define the unit tangent vector

$$\tau(z) := \partial_z \Phi(t(z), \ell(s)).$$

The curvature $\kappa(z)$ and unit normal vector $n(z)$ are defined by

$$\partial_z \tau(z) = \kappa(z) n(z).$$

The torsion $T(z)$ and binormal vector $b(z)$ are then defined through the Frenet–Serret relation:

$$\partial_z n(z) = -\kappa(z) \tau(z) + T(z) b(z).$$

For any initial particle

$$x = \ell(s) + Z(0, r_1, r_2) \tau(0) + r_1 n(0) + r_2 b(0),$$

the flow map $\Phi(t, x)$ can be uniquely expressed (for sufficiently small r_1, r_2) as

$$(3) \quad \begin{aligned} \Phi(t, x) &=: \Phi(t, s, r_1, r_2) \\ &= \Phi(t, \ell(s)) + Z(t, r_1, r_2) \tau(t) + R_1(t, r_1, r_2) n(t) + R_2(t, r_1, r_2) b(t). \end{aligned}$$

Here

$$Z(0, r_1, r_2) = \alpha_1(0)r_1 + \alpha_2(0)r_2, \quad Z(t, 0, 0) = 0,$$

and

$$R_1(0, r_1, r_2) = r_1, \quad R_2(0, r_1, r_2) = r_2,$$

with $\alpha_1(0), \alpha_2(0) \in \mathbb{R}$. Since the Jacobian

$$\frac{\partial(R_1, R_2)}{\partial(r_1, r_2)}$$

is nonzero at $(r_1, r_2) = (0, 0)$, the inverse function theorem implies that, for each fixed $t > 0$ and for sufficiently small $|R_1|, |R_2|$, we may rewrite (3) in terms of

(R_1, R_2) as follows. Let $r_1 = r_1(t, R_1, R_2)$ and $r_2 = r_2(t, R_1, R_2)$ denote the corresponding inverse functions. Then, for any initial particle

$$x = \ell(s) + r_1(t, R_1, R_2) n(0) + r_2(t, R_1, R_2) b(0),$$

we have

$$\begin{aligned} \Phi(t, x) &=: \Phi(t, s, R_1, R_2) \\ (4) \quad &= \Phi(t, \ell(s)) + Z(t, r_1(t, R_1, R_2), r_2(t, R_1, R_2)) \tau(t) \\ &\quad + R_1 n(t) + R_2 b(t). \end{aligned}$$

Note that $\Phi(t, s, R_1, R_2)|_{R_1=R_2=0}$ represents the Lagrangian transport of the vortex axis ℓ . We now simplify the function Z by the expansion

$$(5) \quad Z(t, r_1(t, R_1, R_2), r_2(t, R_1, R_2)) = \alpha_1(t)R_1 + \alpha_2(t)R_2 + \mathcal{O}(R_1^2 + R_2^2),$$

and we interpret Z as describing the time evolution of swirling particles around the vortex axis. We are now in a position to state the following key theorem.

Theorem 1. *The quantities α_1 and α_2 satisfy the following second-order wave equations:*

$$\begin{aligned} \alpha_1''(t) &= \frac{v''(t)}{v(t)} \alpha_1(t) + 2v(t)\kappa'(t) + 4v'(t)\kappa(t), \\ \alpha_2''(t) &= \frac{v''(t)}{v(t)} \alpha_2(t). \end{aligned}$$

Remark 1. *In a separate line of research, Hasimoto's remarkable discovery that the Local Induction Approximation (LIA) reduces to the focusing nonlinear Schrödinger equation revealed a profound connection between filament geometry and dispersive wave dynamics (see [4]). Despite these influential developments, existing theories rely fundamentally on vortex-filament approximations, such as concentrated vorticity, Biot-Savart expansions, LIA truncations, or asymptotic regimes in which the vortex core radius is assumed to be small. Consequently, the emergence of wave phenomena has traditionally been viewed as a feature of singular or nearly singular vortex models. It has therefore remained unclear whether similar wave dynamics arise intrinsically within the full incompressible Euler equations in a smooth, non-filament setting.*

To the best of our knowledge, this paper is the first derivation showing that wave equations governing Lagrangian motion emerge directly from the incompressible Euler equations in a fully smooth setting.

3. PROOF OF THEOREM 1

The key point of the proof is a direct computation of $\partial_{R_1}(\partial_t^2 \Phi \cdot \tau)$ and $\partial_{R_2}(\partial_t^2 \Phi \cdot \tau)$ along the transported curve $\bigcup_t \Phi(t, \ell(s))$. Let us recall the Frenet-Serret formulas:

$$\frac{d}{dz} \begin{pmatrix} \tau \\ n \\ b \end{pmatrix} = \begin{pmatrix} 0 & \kappa & 0 \\ -\kappa & 0 & T \\ 0 & -T & 0 \end{pmatrix} \begin{pmatrix} \tau \\ n \\ b \end{pmatrix}.$$

By combining the Frenet–Serret formulas with (4) and (5), we obtain the expansions

$$(6) \quad \begin{cases} \partial_z \Phi = \tau + R_1(Tb - \kappa\tau) - R_2Tn \\ \quad + (R_1\alpha_1 + R_2\alpha_2)\kappa n + (R_1\partial_z\alpha_1 + R_2\partial_z\alpha_2)\tau + \mathcal{O}(R_1^2 + R_2^2), \\ \partial_{R_1} \Phi = n + \alpha_1\tau + \mathcal{O}(|R_1| + |R_2|), \\ \partial_{R_2} \Phi = b + \alpha_2\tau + \mathcal{O}(|R_1| + |R_2|), \end{cases}$$

where $\mathcal{O}(\cdot)$ denotes Landau's notation. Equivalently, (6) can be written in matrix form as

$$\begin{pmatrix} \partial_z \Phi \\ \partial_{R_1} \Phi \\ \partial_{R_2} \Phi \end{pmatrix} = \begin{pmatrix} (1 - \kappa R_1) + (R_1\partial_z\alpha_1 + R_2\partial_z\alpha_2) & -R_2T + (R_1\alpha_1 + R_2\alpha_2)\kappa & R_1T \\ \alpha_1 & 1 & 0 \\ \alpha_2 & 0 & 1 \end{pmatrix} \begin{pmatrix} \tau \\ n \\ b \end{pmatrix}$$

$$=: \begin{pmatrix} A & B & C \\ \alpha_1 & 1 & 0 \\ \alpha_2 & 0 & 1 \end{pmatrix} \begin{pmatrix} \tau \\ n \\ b \end{pmatrix},$$

where

$$\begin{cases} A = (1 - \kappa R_1) + (R_1\partial_z\alpha_1 + R_2\partial_z\alpha_2), \\ B = -R_2T + (R_1\alpha_1 + R_2\alpha_2)\kappa, \\ C = R_1T. \end{cases}$$

We omit higher-order terms since we will eventually take the limit $R_1, R_2 \rightarrow 0$. The corresponding inverse matrix is

$$(7) \quad \begin{pmatrix} \tau \\ n \\ b \end{pmatrix} = \frac{1}{D} \begin{pmatrix} 1 & -B & -C \\ -\alpha_1 & A - C\alpha_2 & C\alpha_1 \\ -\alpha_2 & B\alpha_2 & A - B\alpha_1 \end{pmatrix} \begin{pmatrix} \partial_z \Phi \\ \partial_{R_1} \Phi \\ \partial_{R_2} \Phi \end{pmatrix},$$

where $D = A - B\alpha_1 - C\alpha_2$. Moreover, differentiating (6) once more in z and using the Frenet–Serret relations, we obtain

$$\begin{aligned} \partial_z^2 \Phi &= \kappa n - R_1(T^2 + \kappa^2)n + R_1((\partial_z T)b - (\partial_z \kappa)\tau) \\ &\quad - R_2T(-\kappa\tau + Tb) - R_2(\partial_z T)n \\ &\quad + (R_1\partial_z^2\alpha_1 + R_2\partial_z^2\alpha_2)\tau + 2(R_1\partial_z\alpha_1 + R_2\partial_z\alpha_2)\kappa n \\ &\quad + (R_1\alpha_1 + R_2\alpha_2)(\partial_z \kappa)n + (R_1\alpha_1 + R_2\alpha_2)\kappa(-\kappa\tau + Tb) \\ &\quad + \mathcal{O}(R_1^2 + R_2^2). \end{aligned}$$

Consequently,

$$\begin{aligned} \partial_{R_1} \partial_z \Phi \Big|_{R_1=R_2=0} &= Tb - \kappa\tau + \alpha_1\kappa n + \partial_z\alpha_1\tau, \\ \partial_{R_1} \partial_z^2 \Phi \Big|_{R_1=R_2=0} &= -(T^2 + \kappa^2)n + ((\partial_z T)b - (\partial_z \kappa)\tau) \\ &\quad + \partial_z^2\alpha_1\tau + 2(\partial_z\alpha_1)\kappa n + \alpha_1(\partial_z \kappa)n - \alpha_1\kappa(\kappa\tau - Tb), \\ \partial_{R_2} \partial_z \Phi \Big|_{R_1=R_2=0} &= -Tn + \alpha_2\kappa n + \partial_z\alpha_2\tau, \\ \partial_{R_2} \partial_z^2 \Phi \Big|_{R_1=R_2=0} &= -T(-\kappa\tau + Tb) - (\partial_z T)n \\ &\quad + \partial_z^2\alpha_2\tau + 2(\partial_z\alpha_2)\kappa n + \alpha_2(\partial_z \kappa)n - \alpha_2\kappa(\kappa\tau - Tb). \end{aligned}$$

Thus, using the identities obtained above and the orthonormality of the Frenet frame, we have

$$(\partial_{R_1} \partial_z^2 \Phi) \cdot \tau \Big|_{R_1=R_2=0} = -\partial_z \kappa + \partial_z^2 \alpha_1 - \kappa^2 \alpha_1, \quad (\partial_{R_1} \partial_z \Phi) \cdot \tau \Big|_{R_1=R_2=0} = -\kappa + \partial_z \alpha_1,$$

and

$$(\partial_{R_2} \partial_z^2 \Phi) \cdot \tau \Big|_{R_1=R_2=0} = T\kappa + \partial_z^2 \alpha_2 - \kappa^2 \alpha_2, \quad (\partial_{R_2} \partial_z \Phi) \cdot \tau \Big|_{R_1=R_2=0} = \partial_z \alpha_2.$$

On the other hand, since $\partial_t = v \partial_z$ along the vortex axis, the Leibniz rule gives

$$\partial_t^2 \Phi = v^2 \partial_z^2 \Phi + v' \partial_z \Phi,$$

where $v' = \partial_t v$ (and we omit writing the variables for brevity). Recall that the prime notation $'$ denotes differentiation with respect to time t , and that ∂_z denotes differentiation with respect to the arc-length parameter z . Therefore, for $R_1 = R_2 = 0$, we obtain

$$\begin{aligned} -\partial_{R_1}(\nabla p \cdot \tau) &= \partial_{R_1}(\partial_t^2 \Phi \cdot \tau) = (\partial_{R_1} \partial_t^2 \Phi) \cdot \tau \\ &= (-\kappa + \partial_z \alpha_1)v' + (-\partial_z \kappa + \partial_z^2 \alpha_1 - \kappa^2 \alpha_1)v^2 \\ &= -v'\kappa - v^2 \partial_z \kappa + \partial_t^2 \alpha_1 - v^2 \kappa^2 \alpha_1, \\ -\partial_{R_2}(\nabla p \cdot \tau) &= \partial_{R_2}(\partial_t^2 \Phi \cdot \tau) = (\partial_{R_2} \partial_t^2 \Phi) \cdot \tau \\ &= (\partial_z \alpha_2)v' + (T\kappa + \partial_z^2 \alpha_2 - \kappa^2 \alpha_2)v^2 \\ &= v^2 T\kappa + \partial_t^2 \alpha_2 - v^2 \kappa^2 \alpha_2. \end{aligned} \tag{8}$$

Next, we derive complementary identities using the Euler equations. Along the vortex axis we have $\partial_t \Phi = v\tau$, and hence

$$\kappa n = \partial_z^2 \Phi(t(z), \ell(s)) = \partial_z(\partial_t \Phi v^{-1}) = \partial_t^2 \Phi v^{-2} - \partial_t \Phi v' v^{-3}.$$

Consequently,

$$\partial_t^2 \Phi = v^2 \kappa n + v' \tau.$$

Using the Euler equations $\partial_t^2 \Phi = -(\nabla p) \circ \Phi$, we obtain, for $R_1 = R_2 = 0$ (again omitting $\circ \Phi$),

$$\begin{aligned} -\nabla p \cdot \tau &= \partial_t^2 \Phi \cdot \tau = v', \\ -\nabla p \cdot n &= \partial_t^2 \Phi \cdot n = v^2 \kappa, \\ -\partial_z(\nabla p \cdot n) &= \partial_z(v^2 \kappa) = v^2 \partial_z \kappa + 2v'\kappa, \\ -\nabla p \cdot b &= \partial_t^2 \Phi \cdot b = 0. \end{aligned}$$

By the explicit inverse formula (7) and the expansion

$$\begin{aligned} D^{-1} &= 1 - \left((-\kappa + \partial_z \alpha_1) - \alpha_1^2 \kappa - T\alpha_2 \right) R_1 \\ &\quad - \left(\partial_z \alpha_2 - (-T + \alpha_2 \kappa) \alpha_1 \right) R_2 + \mathcal{O}(R_1^2 + R_2^2), \end{aligned}$$

we can write

$$\begin{aligned} \nabla p \cdot \tau &= D^{-1}(\nabla p \cdot \partial_z \Phi) - BD^{-1}(\nabla p \cdot \partial_{R_1} \Phi) - CD^{-1}(\nabla p \cdot \partial_{R_2} \Phi) \\ (\text{pull back}) &= D^{-1} \partial_z(p \circ \Phi) - BD^{-1} \partial_{R_1}(p \circ \Phi) - CD^{-1} \partial_{R_2}(p \circ \Phi). \end{aligned}$$

Hence (omitting $\circ\Phi$) we obtain

$$\begin{aligned} -\partial_{R_1}(\nabla p \cdot \tau) \Big|_{R_1=R_2=0} &= \left((-\kappa + \partial_z \alpha_1 - \alpha_1^2 \kappa - T \alpha_2) \partial_z p - \partial_{R_1} \partial_z p \right. \\ &\quad \left. + \alpha_1 \kappa \partial_{R_1} p + T \partial_{R_2} p \right) \Big|_{R_1=R_2=0} \\ (\text{commuting } \partial_{R_1} \text{ and } \partial_z) &= (-\kappa + \partial_z \alpha_1 - \alpha_1^2 \kappa - T \alpha_2) \partial_z p - \partial_z \partial_{R_1} p \\ &\quad + \alpha_1 \kappa \partial_{R_1} p + T \partial_{R_2} p \\ &=: (RHS). \end{aligned}$$

Remark 2. We can rephrase the commutativity of ∂_{R_1} and ∂_z as

$$[\partial_z, \partial_{R_1}] := \partial_z \partial_{R_1} - \partial_{R_1} \partial_z = 0,$$

where $[\cdot, \cdot]$ denotes the Lie bracket. For previous studies exploiting this property, see Chan–Czubak–Y [1, Section 2.5], Lichtenfelz–Y [8], and Shimizu–Y [13]; for an earlier appearance, see Ma–Wang [9, (3.7)].

Since (along $R_1 = R_2 = 0$, again omitting $\circ\Phi$)

$$\begin{aligned} -\partial_{R_1} p &= -(\nabla p \cdot n) - \alpha_1 (\nabla p \cdot \tau) = v^2 \kappa + v' \alpha_1, \\ -\partial_z \partial_{R_1} p &= \partial_z (v^2 \kappa + v' \alpha_1) = v^2 \partial_z \kappa + 2v' \kappa + v' \partial_z \alpha_1 + \frac{v''}{v} \alpha_1, \\ -\partial_{R_2} p &= -(\nabla p \cdot b) - \alpha_2 (\nabla p \cdot \tau) = v' \alpha_2, \\ -\partial_z \partial_{R_2} p &= \partial_z (v' \alpha_2) = \frac{v''}{v} \alpha_2 + v' \partial_z \alpha_2, \\ -\partial_z p &= -(\nabla p \cdot \tau) = v', \end{aligned}$$

we obtain

$$\begin{aligned} (RHS) &= -(-\kappa + \partial_z \alpha_1 - \alpha_1^2 \kappa - T \alpha_2) v' + v^2 \partial_z \kappa + 2v' \kappa + v' \partial_z \alpha_1 + \frac{v''}{v} \alpha_1 \\ &\quad - \alpha_1 \kappa (v^2 \kappa + v' \alpha_1) - T v' \alpha_2 \\ &= v^2 \partial_z \kappa + 3v' \kappa + \frac{v''}{v} \alpha_1 - v^2 \kappa^2 \alpha_1. \end{aligned}$$

On the other hand, similarly,

$$\begin{aligned} -\partial_{R_2}(\nabla p \cdot \tau) &= (\partial_z \alpha_2 + T \alpha_1 - \alpha_1 \alpha_2 \kappa) \partial_z p - \partial_{R_2} \partial_z p - (T - \alpha_2 \kappa) \partial_{R_1} p \\ (\text{commuting } \partial_{R_2} \text{ and } \partial_z) &= (\partial_z \alpha_2 + T \alpha_1 - \alpha_1 \alpha_2 \kappa) \partial_z p - \partial_z \partial_{R_2} p - (T - \alpha_2 \kappa) \partial_{R_1} p \\ &= -(\partial_z \alpha_2 + T \alpha_1 - \alpha_1 \alpha_2 \kappa) v' + \frac{v''}{v} \alpha_2 + v' \partial_z \alpha_2 \\ &\quad + (T - \alpha_2 \kappa) (v^2 \kappa + v' \alpha_1) \\ &= \frac{v''}{v} \alpha_2 + v^2 T \kappa - v^2 \kappa^2 \alpha_2, \end{aligned}$$

for $R_1 = R_2 = 0$. Combining these identities with (8), we arrive at the coupled closure equations

$$\begin{aligned} (9) \quad -v' \kappa - v^2 \partial_z \kappa + \partial_t^2 \alpha_1 - v^2 \kappa^2 \alpha_1 &= v^2 \partial_z \kappa + 3v' \kappa + \frac{v''}{v} \alpha_1 - v^2 \kappa^2 \alpha_1, \\ v^2 T \kappa + \partial_t^2 \alpha_2 - v^2 \kappa^2 \alpha_2 &= \frac{v''}{v} \alpha_2 + v^2 T \kappa - v^2 \kappa^2 \alpha_2. \end{aligned}$$

Note that $\partial_z \kappa = v^{-1} \kappa'$ since $\partial_t = v \partial_z$ along the vortex axis. Rearranging (9) yields

$$\begin{aligned}\alpha_1'' &= \frac{v''}{v} \alpha_1 + 2v\kappa' + 4v'\kappa, \\ \alpha_2'' &= \frac{v''}{v} \alpha_2.\end{aligned}$$

These are the desired wave equations.

4. NUMERICAL IMPLEMENTATION

In this section, we present a numerical implementation to investigate how the alignment between the vortex axis and the axis of swirling particles is maintained during the time evolution of a vortex ring. In particular, we demonstrate that such alignment cannot be preserved by pure radial expansion alone, and that a nontrivial deformation of the ring plays an essential role. We first prescribe an accelerating transport flow that expands in the radial direction, characterized by a scalar function $\Gamma(t)$ satisfying

$$\Gamma(t_0) = 0, \quad \Gamma(t) > 0, \quad \Gamma'(t) > 0, \quad \Gamma''(t) > 0 \quad \text{for } t \in (t_0, t_1).$$

The time evolution of the ring shape, for $t \in [t_0, t_1]$ and $s \in [0, 1]$, is defined by

$$\Phi(t, s) = \left(R(s, \delta) + \Gamma(t) + \gamma_1(t, s) \right) \begin{pmatrix} \cos 2\pi s \\ \sin 2\pi s \\ 0 \end{pmatrix} + \gamma_2(t, s) \begin{pmatrix} 0 \\ 0 \\ 1 \end{pmatrix}.$$

Here,

$$R(s, \delta) := \frac{(1 + \delta)(1 - \delta)}{2\sqrt{\left((1 - \delta) \cos s\right)^2 + \left((1 + \delta) \sin s\right)^2}}$$

represents the initial ring shape with elliptic radius, where $\delta > 0$ is a small ellipticity parameter. The functions $\gamma_1(t, s)$ and $\gamma_2(t, s)$ describe a time-dependent wavy deformation and are given by

$$\begin{aligned}\gamma_1(t, s) &= \frac{1}{K+1} \sum_{j=0}^J \sum_{k=0}^K \left(c_{jk}^{11} (t - t_0)^{j+1} \sin 2\pi ks + c_{jk}^{12} (t - t_0)^{j+1} \cos 2\pi ks \right), \\ \gamma_2(t, s) &= \frac{1}{K+1} \sum_{j=0}^J \sum_{k=0}^K \left(c_{jk}^{21} (t - t_0)^{j+1} \sin 2\pi ks + c_{jk}^{22} (t - t_0)^{j+1} \cos 2\pi ks \right),\end{aligned}$$

where the coefficients $\{c_{jk}^{\ell m}\}_{jk\ell m} \subset \mathbb{R}$ are treated as learnable parameters. We now give a definition of the axis of swirling particles $\zeta(t, s)$ by

$$(10) \quad \zeta(t, s) := \tau(t, s) - \alpha_1(t, s)n(t, s) - \alpha_2(t, s)b(t, s).$$

On the other hand, the vortex axis $\zeta^*(t, s)$ is defined by

$$\zeta^*(t, s) := \partial_s \Phi(t, s, R_1, R_2) \Big|_{R_1=R_2=0}.$$

Recall that α_1 and α_2 satisfy the following wave-type equations:

$$\alpha_1'' = \frac{v''}{v} \alpha_1 + 2v\kappa' + 4v'\kappa, \quad \alpha_2'' = \frac{v''}{v} \alpha_2,$$

where $v(t, s) := |\partial_t \Phi(t, s)|$ and $\kappa(t, s)$ denotes the curvature of the curve $\cup_t \Phi(t, s)$. For the machine learning implementation, we choose the initial data $\alpha_1(0, s), \alpha_2(0, s), \partial_t \alpha_1(0, s)$, and $\partial_t \alpha_2(0, s)$ so that

$$\frac{\zeta^*(0, s)}{|\zeta^*(0, s)|} \cdot \frac{\zeta(0, s)}{|\zeta(0, s)|} = 1, \quad \partial_t \left(\frac{\zeta^*(t, s)}{|\zeta^*(t, s)|} \cdot \frac{\zeta(t, s)}{|\zeta(t, s)|} \right) \Big|_{t=0} = 0 \quad \text{for } s \in [0, 1].$$

These conditions ensure that the vortex axis and the axis of swirling particles are perfectly aligned at the initial time. If the two axes are not parallel, the resulting rotating flow tends to exhibit shear. From a physical viewpoint, it is therefore natural to assume that the system favors configurations in which these axes remain aligned during the evolution, thereby minimizing shear. Motivated by this consideration, we introduce the following mean absolute directional correlation (MADC) as a functional:

$$\text{MADC} := \frac{1}{t_1 - t_0} \int_{t_0}^{t_1} \int_0^1 \left| \frac{\zeta^*(t, s)}{|\zeta^*(t, s)|} \cdot \frac{\zeta(t, s)}{|\zeta(t, s)|} \right| ds dt,$$

which serves as an objective functional to be maximized. In the numerical implementation, we set

$$\Gamma(t) = 1 - \cos(12\pi t), \quad (t_0 = 1/48, t_1 = 1/24),$$

and adopt the following hyperparameters:

- $\delta = 0.02$ (ellipticity parameter),
- $J = 20$ (number of polynomial terms),
- $K = 10$ (number of Fourier modes).

The time interval $[t_0, t_1]$ is discretized into 32 steps, and the angular parameter interval $[0, 1]$ is discretized into 128 points. For optimization, we employ Bayesian optimization using the Optuna library:

- First 10,000 trials: quasi-Monte Carlo sampling,
- Subsequent 50 trials: Bayesian optimization,
- Parameter bounds: $|c_{jk}^{lm}| \leq 30.0$.

The numerical results are shown in Figures 1 and 2. Qualitatively, the results indicate that maintaining alignment between the vortex axis and the axis of swirling particles throughout the evolution requires the presence of a nontrivial wavy deformation. Conversely, larger values of MADC are obtained only when such wavy deformations are included, indicating that these deformations play a fundamental role in generating the discrepancies captured by the error metric. At the present stage, our analysis remains qualitative. Nevertheless, despite prescribing ten Fourier modes in the Bayesian learning procedure, the representations inferred from the image data consistently indicate that the effective dynamics are dominated by five to six Fourier modes. This observation provides strong evidence that the deformation of the vortex ring is governed by scale-local mechanisms. A central direction for future work is to undertake a detailed qualitative investigation of this scale locality.

Acknowledgments. The author thanks to Professors Susumu Goto, Chun Liu and Yoshikazu Giga for valuable comments. Research of TY was partly supported by the JSPS Grants-in-Aid for Scientific Research 24H00186.

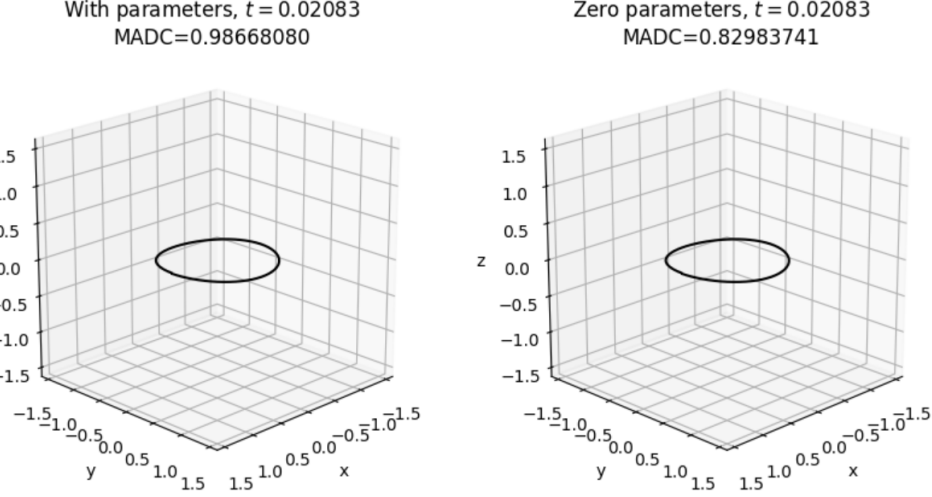


FIGURE 1. Initial vortex rings (the same configuration). Left: Bayesian optimization, Right: $\{c_{jk}^{\ell m}\}_{jk\ell m} = 0$

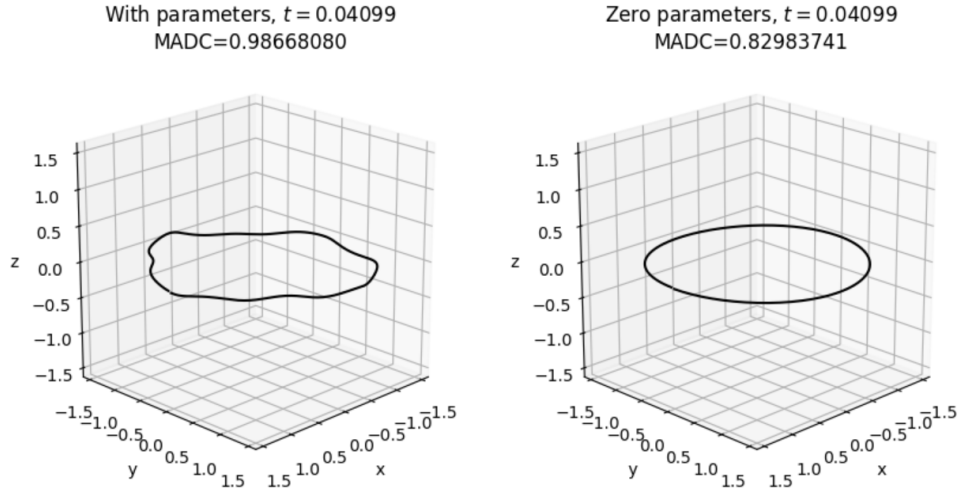


FIGURE 2. Vortex rings at the terminal time. Left: Bayesian optimization, Right: $\{c_{jk}^{\ell m}\}_{jk\ell m} = 0$

REFERENCES

1. C-H. Chan, M. Czubak and T. Yoneda, *An ODE for boundary layer separation on a sphere and a hyperbolic space*, Physica D, **282** (2014) 34-38.
2. S. Goto, *A physical mechanism of the energy cascade in homogeneous isotropic turbulence*, J. Fluid Mech. **605** (2008) 355-366.
3. S. Goto, Y. Saito, and G. Kawahara, *Hierarchy of antiparallel vortex tubes in spatially periodic turbulence at high Reynolds numbers*, Phys. Rev. Fluids **2** (2017) 064603.
4. H. Hasimoto, H. (1972). *A soliton on a vortex filament*, J. Fluid Mech. **51** (1972) 477-485.

5. I.-J. Jeong and T. Yoneda, *Enstrophy dissipation and vortex thinning for the incompressible 2D Navier-Stokes equations*, *Nonlinearity* **34** (2021) 1837.
6. I.-J. Jeong and T. Yoneda, *Vortex stretching and enhanced dissipation for the incompressible 3D Navier-Stokes equations*, *Math. Annal.* **380** (2021) 2041-2072.
7. I.-J. Jeong and T. Yoneda, *Quasi-streamwise vortices and enhanced dissipation for the incompressible 3D Navier-Stokes equations*, *Proceedings of AMS* **150** (2022) 1279-1286.
8. L. Lichtenfelz and T. Yoneda, A local instability mechanism of the Navier-Stokes flow with swirl on the no-slip flat boundary, *J. Math. Fluid Mech.* **21** (2019) 20.
9. T. Ma and S. Wang, *Boundary layer separation and structural bifurcation for 2-D incompressible fluid flows. Partial differential equations and applications*, *Discrete Contin. Dyn. Syst.* **10** (2004) 459-472.
10. R. McKeown, R. Ostilla-Mónico, A. Pumir, M. P. Brenner and S. M. Rubinstein, *Turbulence generation through an iterative cascade of the elliptical instability*, *Sci. Adv.*, **6**, (2020), eaaz2717.
11. Y. Motoori and S. Goto, *Generation mechanism of a hierarchy of vortices in a turbulent boundary layer*, *J. Fluid Mech.* **865** (2019) 1085-1109.
12. Y. Motoori and S. Goto, *Hierarchy of coherent structures and real-space energy transfer in turbulent channel flow*, *J. Fluid Mech.* **911** (2021) A27.
13. Y. Shimizu and T. Yoneda, *Locality of vortex stretching for the 3D Euler equations*, *J. Math. Fluid Mech.*, **25** (2023), 18.
14. T. Tsuruhashi, S. Goto, S. Oka and T. Yoneda, *Self-similar hierarchy of coherent tubular vortices in turbulence*, to appear in *Philosophical Transactions A*.
15. T. Yoneda, S. Goto and T. Tsuruhashi, *Mathematical reformulation of the Kolmogorov-Richardson energy cascade in terms of vortex stretching*, *Nonlinearity* **34** (2021) 1837.

GRADUATE SCHOOL OF ECONOMICS, HITOTSUBASHI UNIVERSITY, 2-1 NAKA, KUNITACHI, TOKYO 186-8601, JAPAN

Email address: t.yoneda@r.hit-u.ac.jp